Challenge Journal of Structural Mechanics

Resolution of torsional effects in prestressed girders of railway viaducts through use of diaphragms or proper section design

Niyazi Özgür Bezgin *

Deparment of Civil Engineering, İstanbul University, 34320 İstanbul, Turkey

ABSTRACT

Need for elevated railways may arise when capacity of bus transit and light rail transit that share the right of way with roadways becomes insufficient and the cost of railways with dedicated right of ways such as underground railways becomes costly. A similar need arose in the city of Makah and in 2010 an 18-km long; elevated railway transit service began servicing between the districts of Mina, Arafat and Muzdalifah. Today the two-track elevated system serves along the route constructed by posttensioned 25-m long U-sections spanning between piers. This paper presents the analytical studies and the finite element model of an alternative 30-m long pretensioned boxed-section evaluated during the tender stage. Following a comparison with the applied choice, benefits of the U-section with respect to the analyzed alternative will be discussed.

ARTICLE INFO

Article history:
Received 12 August 2015
Accepted 28 September 2015

Keywords:
Railways
Elevated railways
Prefabrication
Prestressing
Viaducts

1. Introduction

Makah is an important religious city with a population of 1.6 million residents. The roadway networks between the religious sites became insufficient under the increased transportation demand especially during the holy month of Hajj and months of Umrah. Population of the city increase roughly 2 million during the month of Hajj. The capacity of the roadway between the holy sites of Mina and Arafat was insufficient to supply the increased demand during the holy months and therefore an increased mass transit capacity through a two-track elevated railway was proposed.

As a part of the Makah Metro, the 18 km long section between Mina and Arafat serves along 9-stations. Fig. 1 shows the plan of the route that opened to service in November 2010 (Wikipedia, 2015).

The 12-wagon trains serving along the tracks can carry 250 passengers in each wagon and with 24-trips per hour; the capacity of the railway is 72,000 passengers per hour (Railway Technology, 2015).

The route supported by a viaduct today is composed mainly of 25-m long prestressed sections. However during the tender stage of the project an alternative viaduct composed of 30 m long sections were evaluated to reduce the number of spans and the number of supporting piers. This study presents a 3D finite element model of the proposed section and structural analysis for the effects of the expected torsion along the section (Bezgin, 2008).

2. The Proposed Cross-Section of the Track

Fig. 2 presents the section evaluated in the 2008 tender study. The evaluated section is composed of a prefabricated section with 0.95 m^2 cross section area and a shaded cast in place slab section with 1 m^2 cross section area that is composite with the prefabricated section (Bezgin, 2008). Figure also shows the vertical location of the center of gravity of the composite section.

The moment of inertia of the prefabricated section and the composite section is 0.24 m^4 and 0.58 m^4 respectively. Mass of the 30 m long prefabricated girder and the composite girder with the cast in place deck is 71 Ton and 146 Ton respectively.

* *Corresponding author*. Tel.: +90-212-4737070 ; E-mail address: ozgur.bezgin@istanbul.edu.tr (N. Ö. Bezgin)

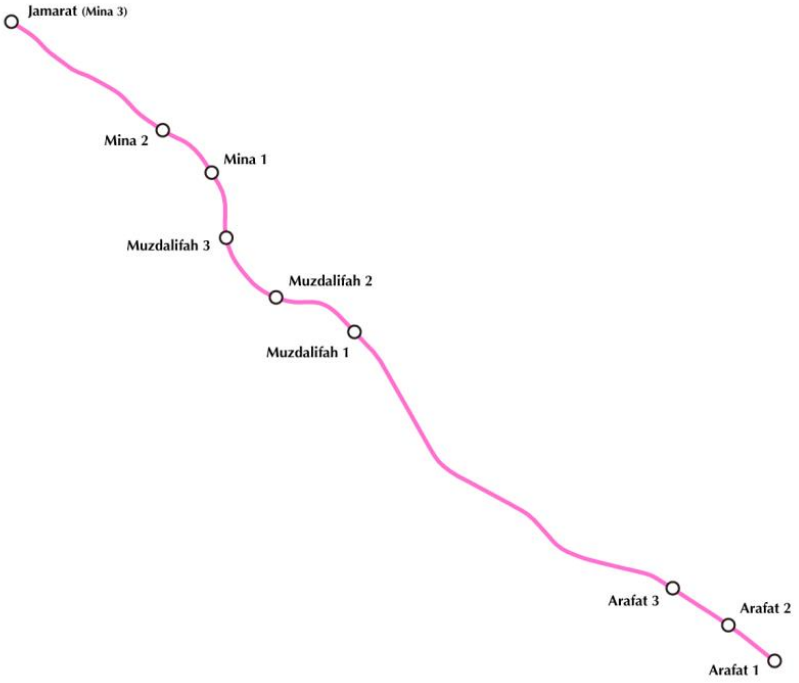

Fig. 1. Elevated railway plan of the proposed route (Wikipedia, 2015).

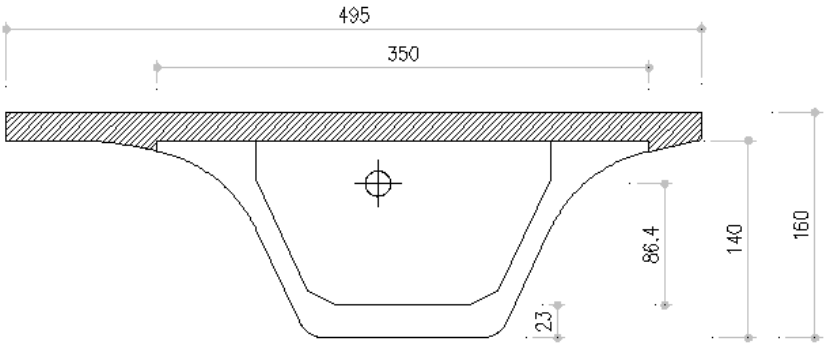

Fig. 2. Evaluated cross-section.

3. Loads Acting on the Girder

Fig. 3 shows the general attributes of the designed track. The track that is supported by special L-shaped beams cast in place with the slab is flanked to the left by a cable duct that also serves as a platform.

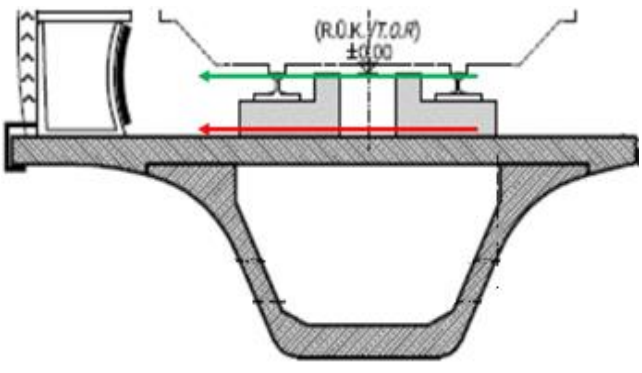

Fig. 3. General attributes of the track cross-section.

The design speed of the train is 80 km/h and the design static axle load is 17 Ton. Dynamic load factor is considered as 1.3 and the quasi-static estimate of the dynamic wheel load is 11 Ton (Lichtberger, 2011). For a design radius of 500 m, the centripetal loads are estimated as 5.3 Ton/axle. Additional dead load on the composite girder due to rail-beams, cable ducts and railings is 0.6 Ton/m. Eq. (1) represents the value of the equivalent load couple acting at the ends of the cross-section, representing the moment generated as the lateral loads applied at the railheads induce a longitudinal bending action at the slab surface 25 cm below.

$$F * 4.9\,m = 5400\,kg * 0.25\,m$$

$$\rightarrow F = 276\,kg = 0.3\,Ton\,, \qquad (1)$$

Fig. 4 shows the vertical and lateral axle loads applied onto the girder. Longitudinal loads due to acceleration and deceleration is estimated at 15% of the vertical loads (Lichtberger, 2011).

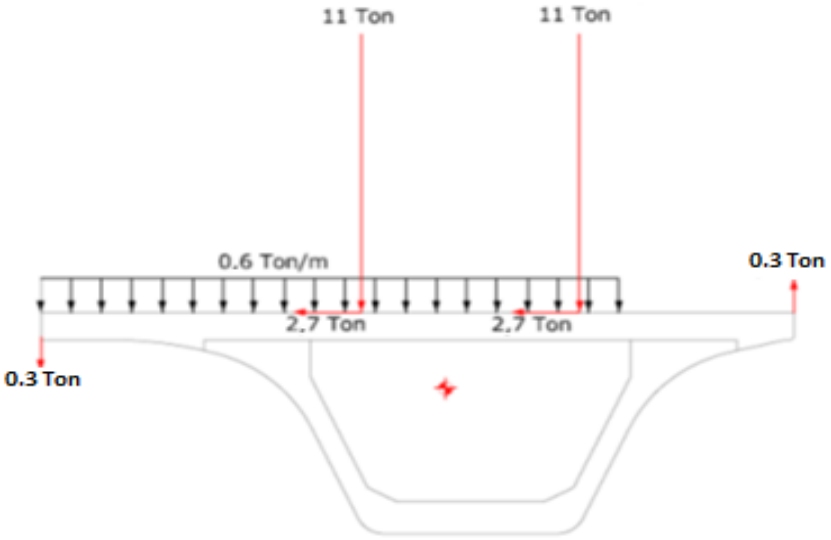

Fig. 4. Application of vertical and lateral loads on the cross section (Bezgin, 2008).

4. Finite Element Analysis of the Prestressed Girder Under the Action of Estimated Loads

A long-term prestressing loss under the humidity and temperature conditions of Makah was estimated at 35%. Fig. 5 shows the perspective view of the design prestressed girder with estimated initial 140 kN initial prestressing force. Using the linear and elastic analysis capability of the SAP2000 program, the prestressing forces were introduced at the respective nodes into the section along the transfer lengths of the prestressing wires as shown in Fig. 6. The model was generated by 8-node linear solid elements. The estimated prestressed force is introduced into the section as shown in Fig. 6 along a transfer length of 130 cm through count-74, 1.6 cm diameter wires with 1800 MPa tensile strength (PCI, 1992).

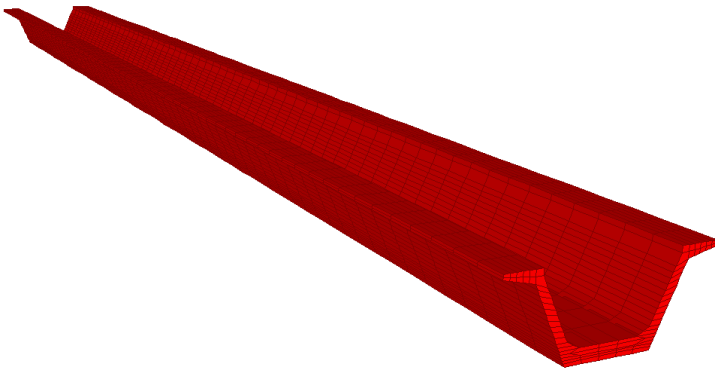

Fig. 5. Perspective view of the prestressed section model (Bezgin, 2008).

Fig. 6. Prestressing forces introduced into the section gradually from its ends (Bezgin, 2008; PCI, 1992).

Under the initial prestressing force, a maximum 2.7 cm camber with a deflection to span ratio L/1100 occurs in the girder as shown in Fig. 7.

Following the placement of the prestressed girder between the piers, cast in place slab is placed, which is modeled as shown in Fig. 8.

After the prestressing losses and the added weight of the cast in place slab, camber is reduced to 0.9 cm with a ratio to girder span of $L/3300$.

Under the action of the axle loads shown in Fig. 9, the net deflection shown in Fig. 10 is 0.75 cm with a ratio to girder span of $L/4000$.

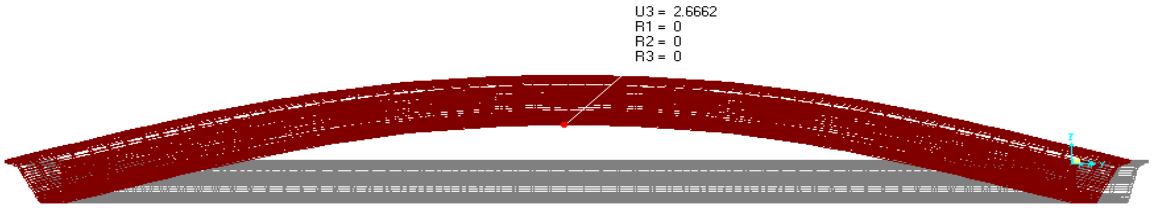

Fig. 7. Inverse camber due to prestressing (Bezgin, 2008).

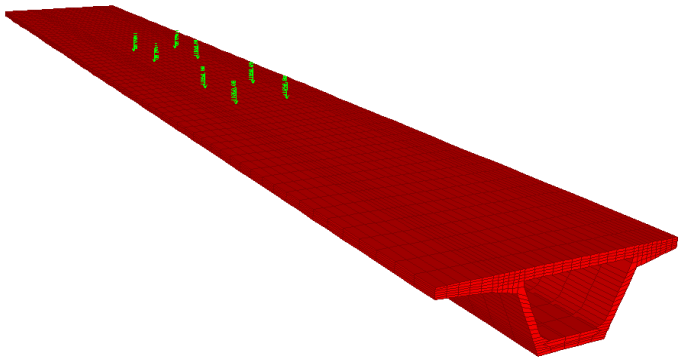

Fig. 8. Cast in place slab and the application of axle loads at the midspan (Bezgin, 2008).

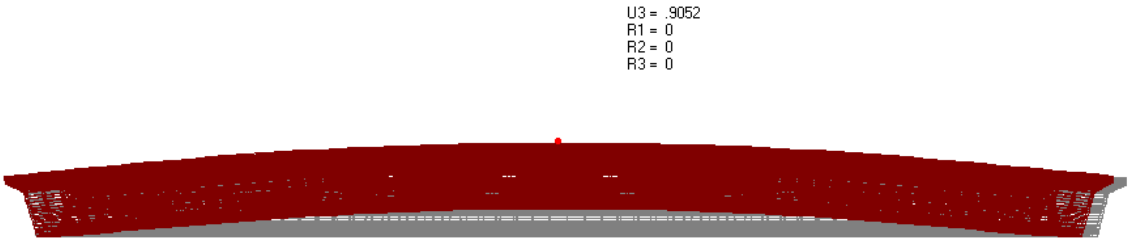

Fig. 9. Remaining inverse camber after the placement of cast in place slab and prestressing losses (Bezgin, 2008).

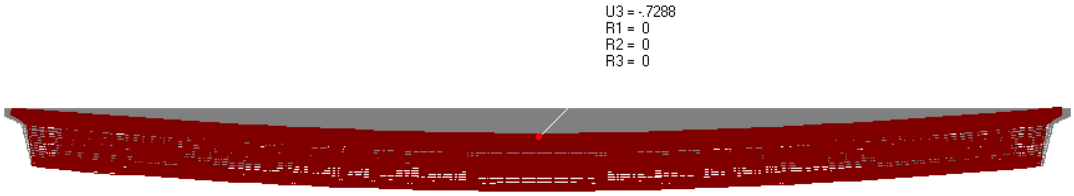

Fig. 10. Net deflection after the addition of the dynamic live loads due to wheel loads (Bezgin, 2008).

Fig. 11 shows the model under the application of the lateral loads that occur at the curvatures along the route in addition to the vertical loads shown in Fig. 8.

The induced torsion distorts the section as shown in Figs. 12-14 shows the distribution of torsional tensile stresses, maximum values of which can be as high as 5 MPa that can crack the C40 grade concrete section. The vertical displacement of the left and right sides of the section at mid-span are 1.3 cm and 0.5 cm respectively. However, since the section is likely to have cracked at these levels of stresses, the displacements and the accompanying torsional rotations are expected to be higher.

Diaphragms placed perpendicularly to the longitudinal axis of the girder can be used to limit the development of torsional distortions and thus the development of torsional stresses along the girder. With 30 cm thick count-4 diaphragms placed at the girder supports, at $L/3$ and $2L/3$ of the span length (L) reduced the vertical displacement at the left and right sides of the mid-span cross section to 0.13 cm and 0.05 cm respectively. Fig. 15 shows the perspective of the prestressed girder with the diaphragms. Fig. 16 shows that the torsional tensile stresses observed in Fig. 14 are drastically reduced due to the presence of the diaphragms resisting distortion due to torsion.

5. Conclusion

Following the tender stage, the owner of the project elected to apply the 25 m long posttensioned girder solution, the cross-section for which is shown in Fig. 17. The section that is fully prefabricated has a cross section area of 2.2 m^2 and a reduced moment inertia that is roughly 70% of the proposed section. Fig. 18 shows the double track cross section and Fig. 19 shows a perspective where the two tracks diverge.

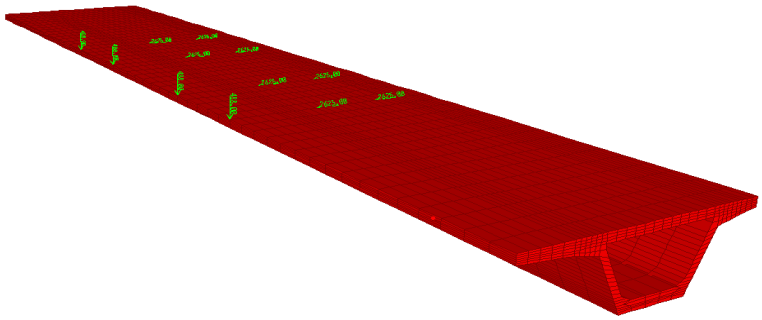

Fig. 11. Application of the lateral and torsional loads in addition to the vertical loads (Bezgin, 2008).

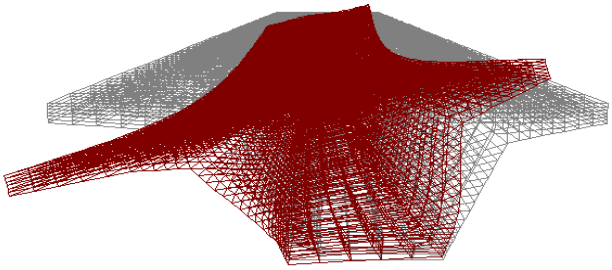

Fig. 12 . Perspective view of torsional distortion along the girder (Bezgin, 2008).

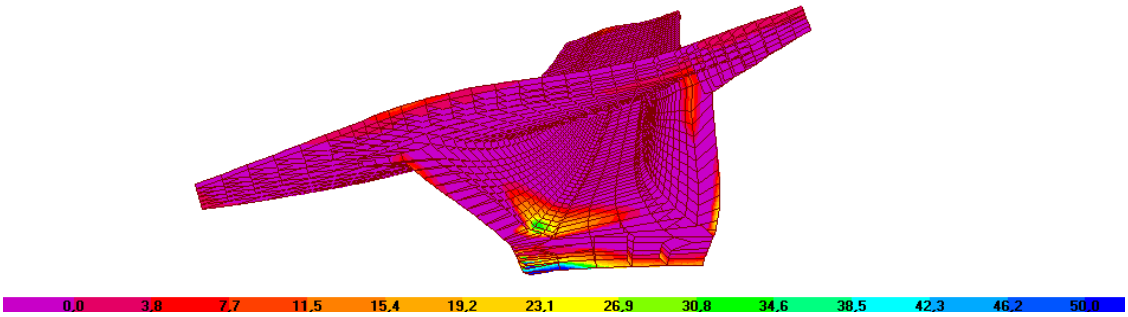

Fig. 13. Tensile stresses due to torsion at the ends of the girder (Bezgin, 2008).

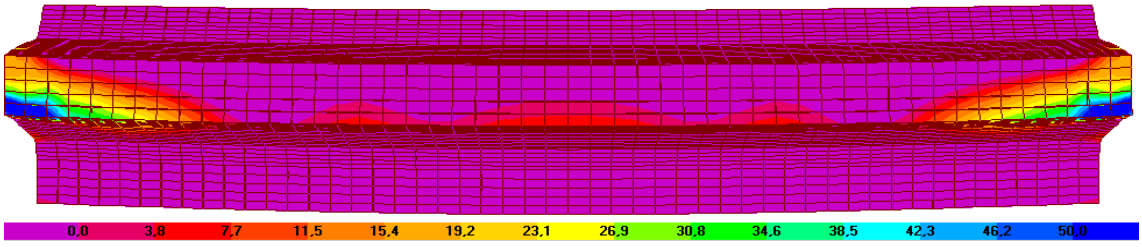

Fig. 14. Tensile stresses due to torsion along the bottom of the girder (Bezgin, 2008).

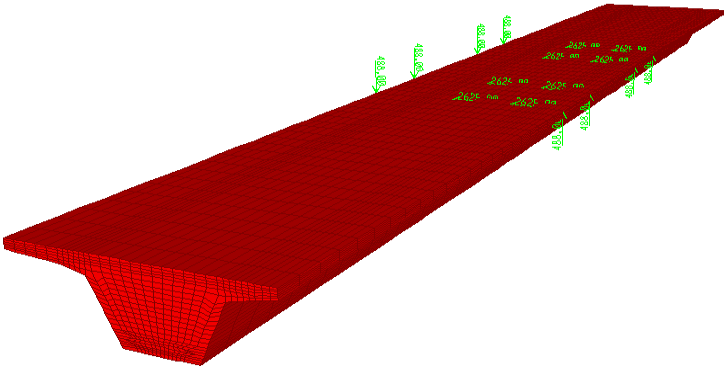

Fig. 15. Use of diaphragms at the supports, at $L/3$ and $2L/3$ distances along the span (L).

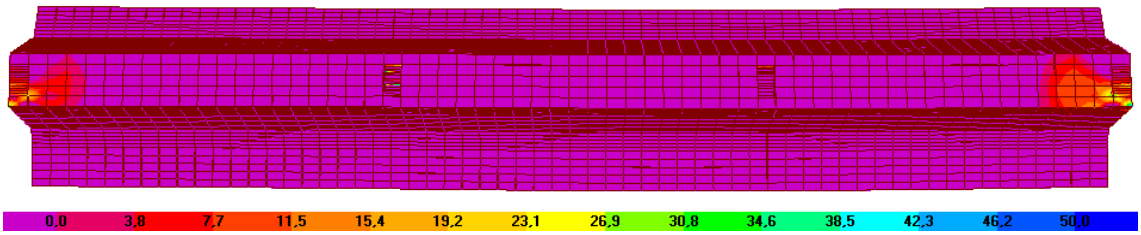

Fig. 16. Reduced torsional stresses with the use of diaphragms (Bezgin, 2008).

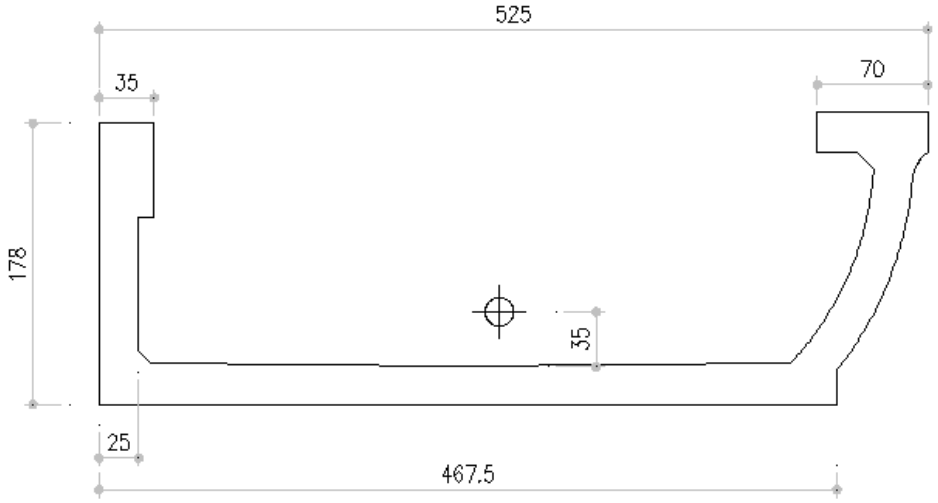

Fig. 17. Preferred section and its center of gravity (Bezgin, 2008).

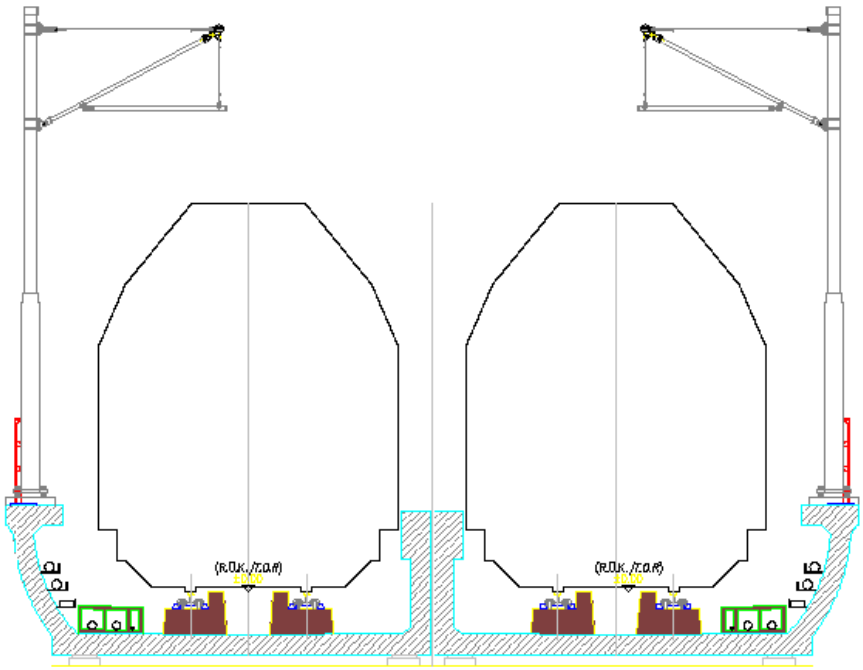

Fig. 18. Cross-section of the two-track railway with the preferred cross-section (PCI, 1992).

Although the elected cross section is heavier and has a lower bending stiffness with a need for increased number of spans along the route it has some significant benefits that the evaluated section does not have. Firstly, the elected solution encompasses the track structure thereby suppressing the emanation of noise due to wheel and track interaction.

Secondly, the elected section lowers the elevation of the tracks thereby reducing the height of the elevated stations from the ground level. Thirdly, the section is fully prefabricated including the rail beams, thereby eliminating the site work required for the cast in place operations, which would be particularly difficult under the high temperatures of the project site.

Fig. 19. A perspective view of the route (PCI, 1992).

Lastly, the problem of torsion is resolved within the geometry of the section. According to Fig. 17, the center of gravity of the section is 35 cm above the top face of the bottom part of the girder. The rail beams are also fabricated with the section such that the top elevation of the rails is also 35 cm above the top face of the bottom part of the girder. Therefore, the lateral forces applied at the railheads pass directly through the center of gravity of the section thus preventing torsion.

In Fig. 3 of the evaluated section, the lateral forces are transferred to the top of the slab via the rail beams at a location that is 50 cm above the center of gravity of the section. The generated torsion is resisted through the diaphragms. However, rather than generating and resisting torsion, it is better to use a design that prevents torsion in the first place.

REFERENCES

Bezgin NÖ (2008). Makah, Mina-Arafat Elevated Railway Track Design Report. Yapı Merkezi Prefabrication Inc., İstanbul, Turkey.

Lichtberger B (2011). Track Compendium. Eurail Press, Hamburg, Germany.

PCI (1992). PCI Design Handbook. Precast/Prestressed Concrete Institute, Chicago, Illinois, USA.

Railway Technology (2013). http://www.railway-technology.com/projects/al-mashaaer-al-mugad. Al Mashaaer Al Mugaddassah Metro Project, Saudi Arabia. Downloaded on 17-01-2013.

Redgage (2014). http://www.redgage.com/photos/mohamadi/makkah-mecca-metro-railway.html. Makkah (Mecca) Metro Railway. Downloaded on 6-11-2014.

Wikipedia (2015). http://en.wikipedia.org/wiki/Al_Mashaaer_Al_Mugaddassah_Metro. Al Mashaaer Al Mugaddassah Metro Project, Saudi Arabia. Downloaded on 20-03-2015.